

PET Imaging of Norepinephrine Transporter–Expressing Tumors Using ⁷⁶Br-*meta*-Bromobenzylguanidine

Shigeki Watanabe¹, Hirofumi Hanaoka², Ji Xin Liang¹, Yasuhiko Iida², Keigo Endo³, and Noriko S. Ishioka¹

¹Medical Radioisotope Application Group, Quantum Beam Science Directorate, Japan Atomic Energy Agency, Takasaki, Gunma, Japan; ²Department of Bioimaging Information Analysis, Gunma University Graduate School of Medicine, Maebashi, Gunma, Japan; and ³Department of Diagnostic Radiology and Nuclear Medicine, Gunma University Graduate School of Medicine, Maebashi, Gunma, Japan

Meta-iodobenzylguanidine (MIBG) labeled with ¹²³I or ¹³¹I has been widely used for the diagnosis and radiotherapy of norepinephrine transporter (NET)–expressing tumors. However, ¹²³I/¹³¹I-MIBG has limitations for detecting small lesions because of its lower spatial resolution than PET tracers. In this study, *meta*-bromobenzylguanidine (MBBG) labeled with ⁷⁶Br (half-life, 16.1 h), an attractive positron emitter, was prepared and evaluated as a potential PET tracer for imaging NET-expressing tumors. **Methods:** ⁷⁶Br-MBBG was prepared by a halogen-exchange reaction between the ⁷⁶Br and iodine of non-radioactive MIBG. The stability of MBBG was evaluated in vitro and in vivo by high-performance liquid chromatography analysis. Cellular uptake studies with or without NET inhibitors were performed in NET-positive PC-12 cell lines. Biodistribution studies were performed in PC-12 tumor-bearing nude mice by administration of a mixed solution of MBBG, MIBG, and ¹⁸F-FDG. The tumor was imaged using ⁷⁶Br-MBBG and ¹⁸F-FDG with a small-animal PET scanner. **Results:** MBBG was stable in vitro, but some time-dependent dehalogenation was observed after administration in mice. MBBG showed high uptake in PC-12 tumor cells that was significantly decreased by the addition of NET inhibitors. In biodistribution studies, MBBG showed high tumor accumulation (32.0 ± 18.6 percentage injected dose per gram at 3 h after administration), and the tumor-to-blood ratio reached as high as 54.4 ± 31.9 at 3 h after administration. The tumor uptake of MBBG correlated well with that of MIBG ($r = 0.997$) but not with that of ¹⁸F-FDG. ⁷⁶Br-MBBG PET showed a clear image of the transplanted tumor, with high sensitivity, which was different from the lesion shown by ¹⁸F-FDG PET. **Conclusion:** ⁷⁶Br-MBBG showed high tumor accumulation, which correlated well with that of MIBG, and provided a clear PET image. These results indicated that ⁷⁶Br-MBBG would be a potential PET tracer for imaging NET-expressing neuroendocrine tumors and could provide useful information for determining the indications for ¹³¹I-MIBG therapy.

Key Words: PET; norepinephrine transporter (NET)–expressing tumor; ⁷⁶Br-*meta*-bromobenzylguanidine (⁷⁶Br-MBBG); ¹²³I/¹³¹I-MIBG

J Nucl Med 2010; 51:1472–1479
DOI: 10.2967/jnumed.110.075465

M*eta*-iodobenzylguanidine (MIBG) is a functional analog of norepinephrine and specifically taken up by the norepinephrine transporter (NET) (1,2). Because of this uptake mechanism, ¹²³I- or ¹³¹I-labeled MIBG has been widely used for the diagnosis of NET-expressing neuroendocrine tumors, such as pheochromocytoma, paraganglioma, carcinoid tumor, medullary thyroid carcinoma, and neuroblastoma (3). MIBG labeled with ¹³¹I has also been used for systemic radionuclide therapy of NET-expressing tumors (4–6). ¹³¹I-MIBG therapy is a generally safe and reasonably well-tolerated treatment option and confers symptomatic benefits in patients with NET-expressing neuroendocrine tumors. One of the keys to the success of ¹³¹I-MIBG therapy is the selection of a good responder. The tumor accumulation level of ¹³¹I-MIBG is one of the most important factors, and small tumors or early metastases are considered to respond better than large tumors or cases of advanced disease. However, ¹²³I/¹³¹I-MIBG is not useful for quantifying the tumor accumulation level and has some limitations for detecting small lesions and unexpected metastasis because of its lower-spatial-resolution PET tracers.

¹⁸F-FDG, the main PET tracer in oncology, also has been used for imaging neuroendocrine tumors and can detect tumors with high sensitivity (7–9). ¹⁸F-FDG is useful for imaging poorly differentiated tumors and can identify ¹²³I/¹³¹I-MIBG–negative lesions. On the other hand, well-differentiated neuroendocrine tumors are usually characterized by a slow-growth pattern and low ¹⁸F-FDG sensitivity. Because the accumulation pattern of ¹⁸F-FDG is different from that of MIBG (10,11), it is difficult to use ¹⁸F-FDG for the selection of patients amenable to ¹³¹I-MIBG therapy.

Received Jan. 26, 2010; revision accepted May 10, 2010.
For correspondence or reprints contact: Shigeki Watanabe, 1233
Watanuki-machi, Takasaki, Gunma, 370-1292, Japan.
E-mail: watanabe.shigeki@jaea.go.jp
COPYRIGHT © 2010 by the Society of Nuclear Medicine, Inc.

It is widely acknowledged that PET tracers have many advantages over ^{123}I - or ^{131}I -labeled SPECT tracers, and among the many positron emitters, we selected ^{76}Br (half-life, 16.1 h; β^+ , 57%; electron capture, 43%) because this radionuclide has chemical properties similar to those of iodine (12) and a suitable half-life for tracing the behavior of MIBG analogs. ^{76}Br -meta-bromobenzylguanidine (^{76}Br -MBBG) (Fig. 1) was initially reported as a PET tracer of MIBG analogs for imaging myocardial functions (13,14) and has also been investigated for use in imaging NET-expressing tumors (15). ^{76}Br -MBBG showed a high accumulation in the tumors of nude mice. Thus, ^{76}Br -MBBG would be a potential tracer for imaging NET-expressing tumors. However, the usefulness of ^{76}Br -MBBG has not been fully assessed in a detailed comparison with $^{123}\text{I}/^{131}\text{I}$ -MIBG, and PET has not yet been performed using ^{76}Br -MBBG. In this study, we prepared ^{76}Br -MBBG and evaluated its utility by comparing its stability, cellular uptake, and biodistribution in tumor-bearing mice with that of ^{125}I -MIBG and by comparing its tumor accumulation and detectability in PET with that of ^{18}F -FDG in tumor-bearing mice.

MATERIALS AND METHODS

Chemicals

Enriched ^{76}Se (99.67%) was purchased from Isoflex. $\text{Cu}_2^{\text{nat}}\text{Se}$ was purchased from Sigma-Aldrich. Other reagents were purchased from Wako Pure Chemical Industries. $\mu\text{Bondapak C-18}$ semipreparative columns (length, 300 mm; internal diameter, 7.6 mm) were purchased from Waters. NaH_2PO_4 and acetonitrile were used without further purifications. ^{125}I -MIBG was kindly provided by Fujifilm RI Pharma Co., Ltd. Reversed-phase C-18 thin-layer chromatography plates were purchased from Merck. ^{18}F was produced with a biomedical cyclotron (Cypris HM-18; Sumitomo Heavy Industries, Ltd.), and ^{18}F -FDG was synthesized with an automated apparatus used in our clinical work.

Production of No-Carrier-Added Radiobromine

No-carrier-added ^{76}Br and ^{77}Br , the latter of which is the more suitable radiobromine for basic studies because of its longer half-life (57.1 h), were produced by the procedures reported by Tolmachev et al. (16), with some modifications. Irradiation was performed with proton beams (20 MeV) using an azimuthally varying-field cyclotron at the research facility Takasaki Ion Accelerators for Advanced Radiation Application at the Japan Atomic Energy Agency. Separated radiobromine was trapped into 15 mL of Milli-Q water, which was concentrated to 100–200 μL to pro-

vide for the synthesis of ^{76}Br - or ^{77}Br -labeled MBBG. Radiobromine was characterized by γ -ray spectrometry using a high-purity germanium detector (crystal diameter, 58 mm; length, 67.3 mm) coupled to a multichannel analyzer (EG&G 7700 MCA; Seiko Instruments). The radioactivity was determined by considering the γ -ray energy (^{76}Br , 559 keV; ^{77}Br , 239 keV).

Preparation of MBBG

MBBG was synthesized according to the procedures reported by Loc'h et al. (13), with some modifications. ^{76}Br - or ^{77}Br -labeled MBBG was characterized with analytic reversed-phase high-performance liquid chromatography (RP-HPLC) (mobile phase: 0.01 M NaH_2PO_4 solution:acetonitrile, 85:15; flow rate, 2 mL/min) and reversed-phase thin-layer chromatography (mobile phase: 0.001 M H_3PO_4 solution:acetonitrile, 70:30) with a well-type γ -counter (ARC-7001; Aloka Co., Ltd.). The radiochemical purity was determined by RP-HPLC. Specific activity was also determined by the quantification of nonradioactive MBBG with analytic RP-HPLC.

In Vitro and In Vivo Stabilities

The animals were cared for and treated in accordance with the guidelines of the Animal Care and Experimentation Committee of Gunma University. For in vitro stability, a mixed solution of ^{77}Br -MBBG and ^{125}I -MIBG (20 μL) was added to 180 μL of freshly prepared mouse serum. After incubation for 1, 6, or 24 h at 37°C , the radioactivity of the samples was analyzed by RP-HPLC. For the evaluation of in vivo stability, blood and urine were collected from normal ddY mice at 2, 5, 10, and 30 min and at 1 and 3 h after the intravenous administration of a mixed solution of ^{77}Br -MBBG (2 MBq) and ^{125}I -MIBG (740 kBq). Blood samples were centrifuged at 3,000 rpm for 10 min at 4°C , and then the resultant serum was filtered through a 10-kDa cutoff ultrafiltration membrane (Vivaspin 500; Sartorius). Urine samples were directly filtered through a 10-kDa cutoff ultrafiltration membrane. The radioactivity was analyzed by RP-HPLC under the same conditions described for the preparation of MBBG.

Cellular Uptake In Vitro

The rat pheochromocytoma cell line PC-12 was purchased from the American Type Culture Collection. A mixture of ^{77}Br -MBBG and ^{125}I -MIBG (each 3 kBq) was added to the medium containing PC-12 cells, and then the medium was incubated for 10 min, 30 min, 1 h, 3 h, or 6 h at 37°C . The cell suspension was washed and then centrifuged (3,000 rpm for 3 min). The radioactivity of cell fractions was measured with a well-type γ -counter, and the uptake of ^{77}Br -MBBG and ^{125}I -MIBG was calculated as a percentage of the added activity. The reduced uptake of ^{77}Br -MBBG and ^{125}I -MIBG using desipramine and nisoxetine was also examined, by incubation with 50 mM of the NET inhibitors for 3 h at 37°C . The results are shown as a percentage of the uptake without a NET inhibitor.

Biodistribution Studies in PC-12 Tumor-Bearing Mice

PC-12-bearing mice were prepared by implanting PC-12 tumor cells (5×10^6 cells) into the flanks of BALB/c nude mice. When the tumors were palpable (~ 3 wk after implantation), the mice were used for biodistribution studies. A mixture of ^{77}Br -MBBG (30 kBq) and ^{125}I -MIBG (20 kBq) was administered intravenously to PC-12-bearing mice. Groups of 5 mice were sacrificed at 30 min, 1 h, 3 h, or 6 h after administration of the radiotracers. ^{18}F -FDG (100 kBq) was also administered to PC-12-bearing

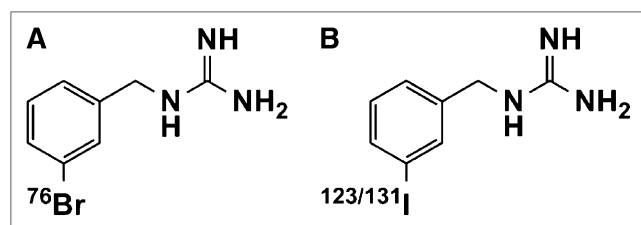


FIGURE 1. Chemical structures of ^{76}Br -MBBG (A) and $^{123}/^{131}\text{I}$ -MIBG (B).

mice, which were then sacrificed at 1 and 3 h after administration. For comparison studies, a mixed solution of ^{77}Br -MBBG (30 kBq), ^{125}I -MIBG (20 kBq), and ^{18}F -FDG (100 kBq) was administered to PC-12-bearing mice ($n = 20$), and the mice were sacrificed at 3 h after administration. In both experiments, the tissues of interest were excised and weighed. Radioactivity was measured using a well-type γ -counter. Briefly, the total radioactivity of ^{18}F and ^{77}Br was measured. Then, the radioactivity of ^{77}Br was determined by measuring at 1 d after the first measurement, because the count of ^{18}F was negligible at that time. The radioactivity of ^{77}Br was calculated using these 2 measurements. Finally, a few weeks later, the radioactivity of ^{125}I was measured. The tissue concentration was expressed as a percentage injected dose per gram. A subset of blood samples was centrifuged to prepare the serum. Finally, the serum epinephrine and norepinephrine levels were measured using a competitive enzyme-linked immunosorbent assay kit (LDN) according to the manufacturer's protocol.

PET Studies with ^{76}Br -MBBG and ^{18}F -FDG

PC-12-bearing mice were intravenously administered 10 MBq of ^{18}F -FDG. The mice were anesthetized with a sodium pentobarbital solution, and PET scans were performed at 1 h after administration using a small-animal PET scanner (Inveon; Siemens) with 20-min emission scanning. Two days after ^{18}F -FDG PET, the tumor-bearing mice were intravenously administered 7 MBq of ^{76}Br -MBBG and also anesthetized with sodium pentobarbital solution. PET scans were then obtained at 1, 3, and 6 h after administration. Semiquantitative analysis was performed for each identified tumor using the tumor-to-background ratio according to a previously described method (17). The target region of interest was placed on the most active area of the tumor mass, and the background region of interest was placed on the lung. The tumor-to-background ratio was finally calculated by dividing the maximum tumor uptake by the mean background uptake. After PET, the tumors were excised and embedded in paraffin ($n = 13$). Consecutive 4- μm -thick sections were prepared from each tumor, and the sections were stained with hematoxylin and eosin. The degree of tumor differentiation was determined using cellularity, necrosis, and a zellballen pattern (a nest of tumor cells surrounded by a highly vascular network; the zellballen pattern is the most prevalent pattern for pheochromocytoma) according to a previously described method (18), with some modifications. Differentiation was classified as follows: well-differentiated was low cellularity, no necrosis, and zellballen pattern; moderately differentiated was moderate cellularity and little or no necrosis; and poorly differentiated was high cellularity and a lot of necrosis.

Statistical Analysis

Data are expressed as mean \pm SD, where appropriate. Results were analyzed using the unpaired t test. Differences were considered statistically significant when the P values were less than 0.05.

RESULTS

Production of No-Carrier-Added ^{76}Br and Synthesis of ^{76}Br -MBBG

In this study, we prepared 250–550 MBq of no-carrier-added ^{76}Br and 30–70 MBq of no-carrier-added ^{77}Br for the synthesis of MBBG (radionuclide purity, $>99\%$). ^{76}Br -MBBG (20–30 MBq) was synthesized with an average labeling efficiency of 44%. The radiochemical purity

was more than 97% in all experiments. The specific activity of ^{76}Br -MBBG was estimated to be more than 18.6 GBq/ μmol .

In Vitro and In Vivo Stability

After incubation in murine serum for 24 h at 37°C, more than 95% of ^{77}Br -MBBG existed in an intact form (Fig. 2). ^{125}I -MIBG was also stable under the same conditions (data not shown).

Analytic RP-HPLC of blood samples showed that more than 90% of radioactivity was attributable to intact ^{77}Br -MBBG, and no free ^{77}Br was observed at 2 min after administration (Fig. 3). Over time, the percentage of total radioactivity attributable to ^{77}Br -MBBG decreased and that attributable to free ^{77}Br increased. In the case of ^{125}I -MIBG, free ^{125}I was already present at 2 min, and it accounted for 60% of total radioactivity at 10 min. In the urine analysis, no free ^{77}Br was observed until 1 h, whereas free ^{125}I was observed in urine at 2 min (data not shown).

Tumor Cellular Uptake

The uptake of ^{77}Br -MBBG increased in a time-dependent manner and reached a plateau at 3 h, but it was slightly lower than the uptake of ^{125}I -MIBG at all time points (Fig. 4A). In the presence of the NET inhibitors desipramine or nisoxetine, uptake of ^{77}Br -MBBG was significantly decreased to less than 40% of the control value (Fig. 4B) ($*P < 0.01$).

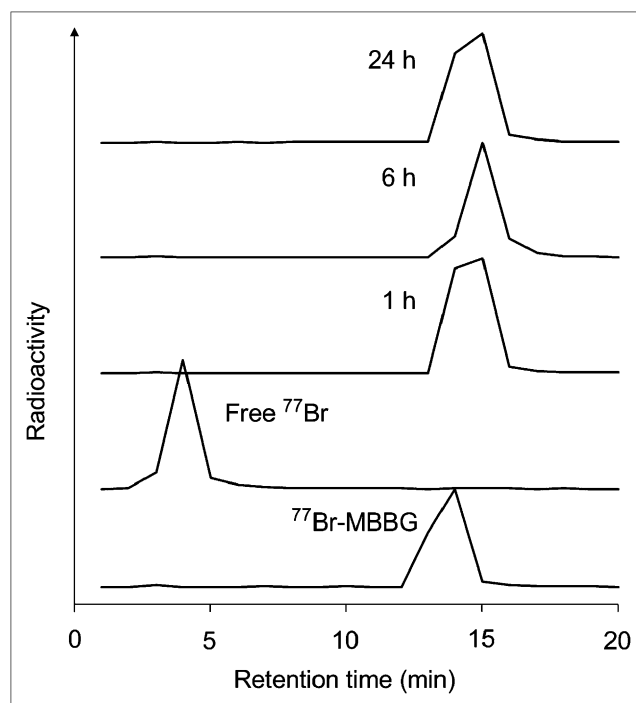


FIGURE 2. Radioactivity profiles of ^{77}Br -MBBG after incubation in murine serum at 37°C for 1, 6, and 24 h. Retention times of ^{77}Br -MBBG and free ^{77}Br were 14–15 min and 4 min, respectively.

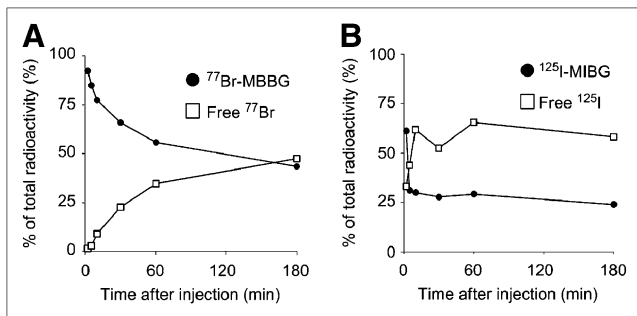


FIGURE 3. Radioactivity profiles in blood after administration of ^{77}Br -MBBG (A) and ^{125}I -MIBG (B) to mice. Blood was drawn from heart of mice at 2, 5, 10, and 30 min and at 1 and 3 h after administration and analyzed by RP-HPLC. Results are shown as percentage of total radioactivity in blood.

Biodistribution Studies

In biodistribution studies with PC-12 tumor-bearing mice, high accumulation of ^{77}Br -MBBG was observed in the transplanted tumor and other NET-positive organs, such as the heart and adrenal glands (Table 1). Biodistribution of ^{77}Br -MBBG was comparable to that of ^{125}I -MIBG and slightly higher than that of ^{125}I -MIBG in the NET-expressing organs (tumor, heart, and adrenal glands). The tumor uptake of ^{77}Br -MBBG peaked at 3 h after administration (32.0 ± 18.6 percentage injected dose per gram), resulting in high tumor-to-blood and tumor-to-muscle ratios of 54.4 ± 31.9 and 33.1 ± 24.9 , respectively. ^{18}F -FDG also showed accumulation and retention in the tumor (Table 2).

The tumor uptake of ^{77}Br -MBBG was well correlated with that of ^{125}I -MIBG ($r = 0.997$) (Fig. 5A), but there was no correlation with ^{18}F -FDG (Fig. 5B). The serum epinephrine and norepinephrine levels ranged from 1.4 to 8.8 ng/mL and from 16.6 to 53.7 ng/mL, respectively, and were not correlated with each other or with the tumor uptake of ^{77}Br -MBBG (data not shown).

PET Studies with ^{76}Br -MBBG and ^{18}F -FDG

Small-animal PET demonstrated that the transplanted PC-12 tumor was successfully imaged at 3 h after admin-

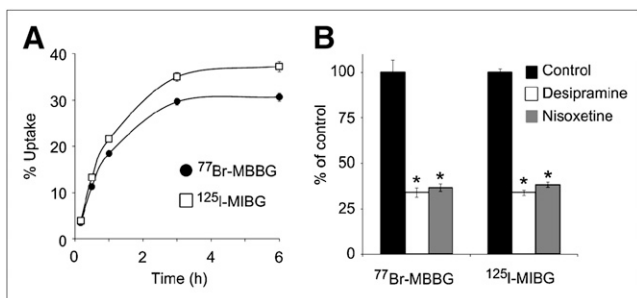


FIGURE 4. Time course of cellular uptake of ^{77}Br -MBBG and ^{125}I -MIBG in PC-12 cells (A), and reduction of uptake of ^{77}Br -MBBG and ^{125}I -MIBG by NET inhibitors (desipramine and nisoxetine) (B). All results are shown as mean \pm SD. $^*P < 0.01$.

istration. High accumulation was also observed at this time point in the bladder, liver, stomach, and intestines and around the throat (Fig. 6), after which ^{76}Br -MBBG was gradually cleared from these nontarget organs. In mouse 1, ^{76}Br -MBBG was able to detect a small tumor (~ 5 mg; lower arrow), which was undetected before PET. On the other hand, ^{18}F -FDG failed to detect an even larger tumor. In mouse 2, 2 tumors showed differential uptake of ^{76}Br -MBBG and ^{18}F -FDG. That is, ^{76}Br -MBBG showed high accumulation in the lower tumor, but ^{18}F -FDG showed high accumulation in the upper tumor. In mouse 3, both ^{76}Br -MBBG and ^{18}F -FDG showed high accumulation in each tumor. The tumors in mouse 2 appeared to be different in color (Fig. 7A). In addition, histopathologic analysis showed that diffuse proliferation of small cells with high cellularity and necrosis was observed in the upper tumor, indicating that it was poorly differentiated (Fig. 7B), and demonstrated a zellballen pattern in the lower tumor, indicating that it was well-differentiated (Fig. 7C). By histologic analysis, 6 of the 13 excised tumors were classified as “well-differentiated,” 3 as “moderately differentiated,” and 4 as “poorly differentiated.” The relationship between ^{18}F -FDG and ^{76}Br -MBBG uptake and differentiation in the tumor is plotted in Figure 7D. Well-differentiated tumors showed ^{76}Br -MBBG–strong and ^{18}F -FDG–weak uptake, and poorly differentiated tumors showed ^{76}Br -MBBG–weak and ^{18}F -FDG–strong uptake.

DISCUSSION

Although the availability of ^{76}Br is currently limited, this situation is expected to change, and ^{76}Br -labeled PET tracers will thus attract increasing attention. Due to the relatively long half-life of ^{76}Br , it may be possible for commercial companies or large facilities to produce ^{76}Br -labeled PET tracer and deliver it to medical facilities. Human studies of some ^{76}Br -labeled tracers have already been performed and showed clear PET images of tumors (19,20), indicating the applicability of ^{76}Br to the clinical phase. The ^{76}Br -MBBG synthesized in this study was of high radiochemical purity and exhibited specific activity (>18.6 GBq/ μmol). Thus, the results indicate that a sufficient quality of ^{76}Br -MBBG can be synthesized for use in clinical applications using no-carrier-added ^{76}Br . Because of these qualities and the relatively long half-life, it would indeed be possible for commercial companies or large facilities to produce the ^{76}Br -MBBG and deliver it to medical facilities for the imaging of NET-positive tumors.

MIBG analogs labeled with other positron emitters have already been reported. The 2 PET nuclides currently available— ^{11}C - and ^{18}F -labeled MIBG analogs—have been investigated in the preclinical phase (21–24). However, the short half-life of ^{11}C is not ideal for tracing MIBG kinetics, and the lower labeling efficiency and complicated synthesis steps of the ^{18}F -labeled MIBG analog may prevent its development for clinical applications. MIBG labeled with a positron-emitting radioiodine, ^{124}I (half-life, 100.2 h; β^+ ,

TABLE 1. Biodistribution and Tumor-to-Organ Ratio of ⁷⁷Br-MBBG and ¹²⁵I-MIBG in PC-12-Bearing Mice

| Tracer/organ | Time after injection | | | |
|-----------------------------|----------------------|---------------|---------------|--------------|
| | 30 min | 1 h | 3 h | 6 h |
| ⁷⁷Br-MBBG | | | | |
| Blood | 0.86 ± 0.11 | 0.83 ± 0.02 | 0.59 ± 0.10 | 0.52 ± 0.03 |
| Liver | 8.39 ± 0.45 | 7.62 ± 0.37 | 3.95 ± 0.37 | 2.30 ± 0.11 |
| Kidney | 2.03 ± 0.28 | 1.62 ± 0.12 | 1.36 ± 0.18 | 1.07 ± 0.17 |
| Intestine | 5.45 ± 0.45 | 4.83 ± 0.16 | 4.93 ± 0.59 | 3.58 ± 0.23 |
| Stomach | 2.24 ± 0.30 | 2.16 ± 0.21 | 2.18 ± 0.58 | 1.43 ± 0.32 |
| Heart | 16.81 ± 1.71 | 13.24 ± 0.95 | 14.16 ± 5.25 | 9.04 ± 0.73 |
| Adrenal | 14.85 ± 3.35 | 12.86 ± 2.57 | 16.50 ± 4.21 | 17.27 ± 4.38 |
| Muscle | 1.11 ± 0.43 | 1.01 ± 0.17 | 1.04 ± 0.24 | 0.75 ± 0.15 |
| Tumor | 20.29 ± 7.50 | 22.00 ± 10.33 | 32.00 ± 18.60 | 23.71 ± 5.91 |
| Tumor-to-blood ratio | 23.4 ± 7.9 | 26.2 ± 12.0 | 54.4 ± 31.9 | 45.2 ± 10.1 |
| Tumor-to-muscle ratio | 20.2 ± 10.1 | 23.1 ± 12.4 | 33.1 ± 24.9 | 33.1 ± 13.5 |
| ¹²⁵I-MIBG | | | | |
| Blood | 1.00 ± 0.14 | 0.91 ± 0.05 | 0.55 ± 0.12 | 0.32 ± 0.04 |
| Liver | 8.52 ± 0.65 | 7.78 ± 0.42 | 4.17 ± 0.42 | 2.23 ± 0.12 |
| Kidney | 2.29 ± 0.33 | 1.69 ± 0.13 | 1.36 ± 0.25 | 0.94 ± 0.19 |
| Intestine | 5.35 ± 0.43 | 4.92 ± 0.23 | 5.39 ± 0.60 | 3.79 ± 0.22 |
| Stomach | 3.20 ± 0.54 | 2.96 ± 0.07 | 3.15 ± 0.58 | 1.95 ± 0.43 |
| Heart | 14.82 ± 1.53 | 11.39 ± 0.74 | 12.52 ± 4.67 | 8.10 ± 0.68 |
| Adrenal | 12.44 ± 1.69 | 9.92 ± 1.78 | 12.62 ± 4.12 | 11.39 ± 3.23 |
| Muscle | 1.02 ± 0.45 | 0.87 ± 0.15 | 0.92 ± 0.23 | 0.63 ± 0.12 |
| Tumor | 16.17 ± 6.15 | 18.11 ± 8.28 | 25.11 ± 14.95 | 19.35 ± 4.94 |
| Tumor-to-blood ratio | 16.2 ± 5.8 | 19.6 ± 8.3 | 46.4 ± 27.4 | 61.4 ± 14.6 |
| Tumor-to-muscle ratio | 17.8 ± 8.8 | 21.7 ± 11.0 | 28.7 ± 20.1 | 32.2 ± 13.3 |

Each value represents mean ± SD of 5 animals. Values are expressed as percentage injected dose per gram of organ except for tumor-to-blood and tumor-to-muscle ratios.

23%; electron capture, 77%), has already been investigated in preclinical and clinical investigations (25,26). However, the longer half-life of ¹²⁴I is not ideal for tracing MIBG kinetics. At the current stage of development, production of ¹²⁴I is too expensive to allow routine clinical application.

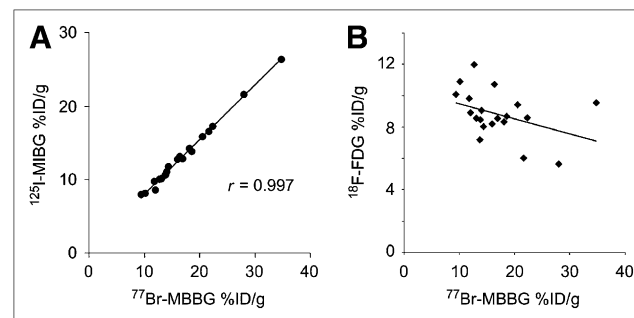
In the present study, the cellular uptake of MBBG was high and significantly reduced by NET inhibitors, indicating that MBBG was specifically taken up by the pheochromocytomas via NET, just like MIBG. However, the uptake of MBBG was slightly lower than that of MIBG, which was attributed to the lower lipophilicity of MBBG, as previously described (22). Stability studies indicated that MIBG was

rapidly metabolized to free iodine, which was excreted into the urine, whereas MBBG was relatively more stable. Thus, a larger amount of MBBG would be able to reach the target tissues without degradation and, consequently, the accumulation of MBBG in the tumor may be higher than that of MIBG. Therefore, although the biodistribution of the 2 tracers is similar, MBBG has advantages both as a PET tracer and from the point of view of tumor accumulation. Our results suggest that ⁷⁶Br-MBBG has the potential to image NET-positive tumors with a higher detectability than ¹²³I-MIBG, which is currently used as the gold standard.

TABLE 2. Biodistribution of ¹⁸F-FDG in PC-12-Bearing Mice

| Organ | Time after administration (h) | |
|-----------|-------------------------------|---------------|
| | 1 | 3 |
| Blood | 0.51 ± 0.04 | 0.22 ± 0.01 |
| Liver | 0.97 ± 0.08 | 0.69 ± 0.05 |
| Kidney | 1.18 ± 0.15 | 0.59 ± 0.08 |
| Intestine | 2.52 ± 0.97 | 1.71 ± 0.10 |
| Heart | 45.04 ± 20.78 | 34.36 ± 14.82 |
| Muscle | 1.70 ± 0.45 | 1.97 ± 0.28 |
| Tumor | 4.40 ± 0.94 | 3.92 ± 1.02 |

Each value represents mean ± SD of 5 animals. Values are expressed as percentage injected dose per gram of organ.

**FIGURE 5.** Comparison of tumor uptake between ⁷⁷Br-MBBG and ¹²⁵I-MIBG (A) and ⁷⁷Br-MBBG and ¹⁸F-FDG (B) at 3 h after administration in PC-12 tumor-bearing mice (*n* = 20). %ID/g = percentage injected dose per gram.

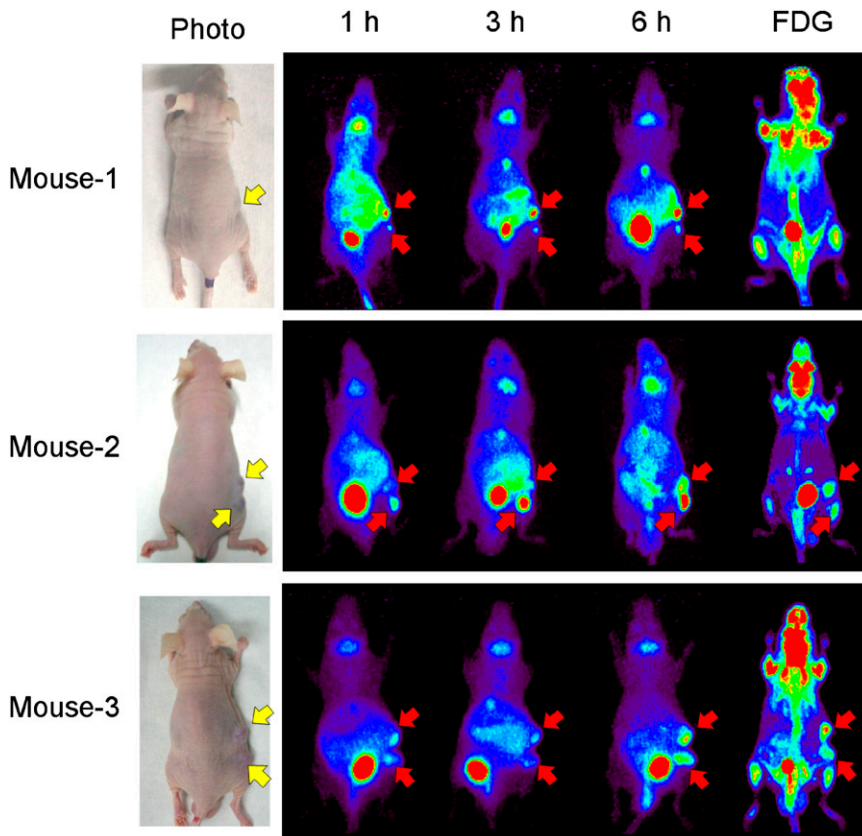


FIGURE 6. PET images of PC-12-bearing mice obtained using ^{76}Br -MBBG and ^{18}F -FDG. Mice were imaged at 1, 3, and 6 h after administration of ^{76}Br -MBBG and at 1 h after administration of ^{18}F -FDG. Yellow arrows indicate position of implanted tumor, and red arrows show tumor detected by PET studies. Tumor weights were as follows—mouse 1: upper, 25 mg, and lower, 5 mg; mouse 2: upper, 110 mg, and lower, 70 mg; and mouse 3: upper, 96 mg, and lower, 53 mg.

In vivo tumor uptake of ^{77}Br -MBBG correlated well with that of ^{125}I -MIBG but not with that of ^{18}F -FDG. ^{76}Br -MBBG would be a powerful tool to estimate the ^{131}I -MIBG accumulation level, which would enable the stratification of patients for their potential response to ^{131}I -MIBG therapy. Recently, several PET tracers specific for neuroendocrine tumors, such as 6- ^{18}F -fluoro-L-dopa (^{18}F -FDOPA) (27–29) and ^{18}F -labeled 6-fluorodopamine (30–33) were developed. ^{18}F -FDOPA is based on the capacity of neuroendocrine tumors to take up L-dihydroxyphenylalanine and to decarboxylate it by aromatic L-amino acid decarboxylase. ^{18}F -FDOPA is a highly sensitive and specific tool that can provide additional independent information for the diagnosis and

localization of benign and malignant pheochromocytomas (28). However, MIBG and ^{18}F -FDOPA images do not completely overlap (29). ^{18}F -6-fluorodopamine shows higher sensitivity than MIBG for the localization of metastatic pheochromocytoma (32,33) but has an accumulation pattern distinct from that of MIBG (30). Thus, these tracers are not sufficient for the selection of responders to ^{131}I -MIBG therapy.

In the present study, the tumor accumulation level of ^{77}Br -MBBG showed a large variation that was not dependent on the serum epinephrine or norepinephrine levels. Although these catecholamines would compete with MBBG uptake, in our study, ^{77}Br -MBBG accumulation in the tumor was not substantially affected by the serum catecholamine level. In our

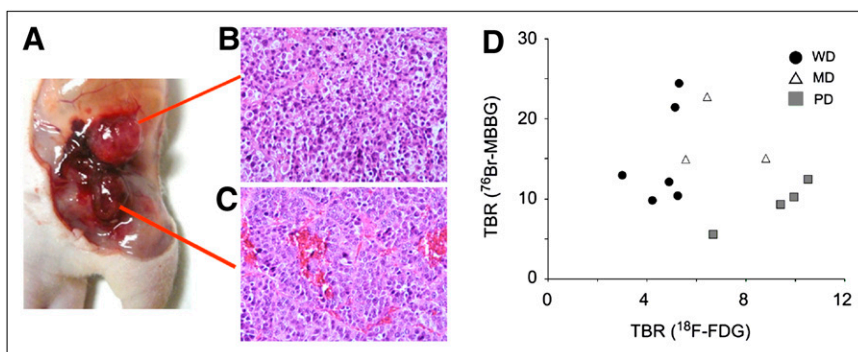


FIGURE 7. Histologic analysis of excised tumors. After PET studies, tumors in mouse 2 were excised (A), and upper (B) and lower (C) tumors were stained with hematoxylin and eosin. Relationship between tumor uptake of ^{18}F -FDG or ^{76}Br -MBBG and tumor differentiation was examined (D). Accumulations of ^{76}Br -MBBG and ^{18}F -FDG were evaluated using tumor-to-background ratio (TBR). MD = moderately differentiated; PD = poorly differentiated; WD = well differentiated.

biodistribution studies, each of the excised tumors had a different color (intensity of redness), which would have been due mainly to the vascular density. Histologic staining of the tumors after PET demonstrated that vascular density reflected the differentiation of individual tumors. Therefore, the variation of tumor differentiation was considered to have contributed to the variation in the accumulation level of ^{76}Br -MBBG.

Our small-animal PET studies demonstrated that ^{76}Br -MBBG could image small tumors (<10 mg) clearly at 3 h after administration. The accumulation patterns of ^{76}Br -MBBG and ^{18}F -FDG in the tumors differed from mouse to mouse and even from lesion to lesion within individual animals. Histologic staining of the tumors indicated that MBBG-strong and ^{18}F -FDG-weak tumors were well differentiated and ^{76}Br -MBBG-weak and ^{18}F -FDG-strong tumors were poorly differentiated (18), which agrees well with the clinical data (34). In the clinical phase, the accumulation patterns of ^{18}F -FDG and MIBG in neuroendocrine tumors have also been shown to differ from lesion to lesion in the same patient (11,29). Thus, ^{76}Br -MBBG PET alone would not be sufficient to detect neuroendocrine tumors, and ^{18}F -FDG PET can sometimes play a complementary role.

An algorithm for the treatment of metastatic pheochromocytoma has been proposed (35). If the progression of the tumor is slower, ^{131}I -MIBG therapy is currently the preferred approach for patients with a positive $^{123}\text{I}/^{131}\text{I}$ -MIBG scan. Because PET using ^{76}Br -MBBG can detect small lesions, it would be useful to determine the indications for ^{131}I -MIBG therapy. A good response is expected if small tumors are treated early. In addition, ^{76}Br -MBBG PET would be a promising method to determine a treatment plan for each patient with NET-expressing tumors. For example, in cases in which ^{76}Br -MBBG detects some—but not all—lesions, ^{131}I -MIBG therapy would not be sufficient and other treatments such as chemotherapy would be needed. A trial of high-dose ^{131}I -MIBG therapy is currently under way (36) and has shown a good therapeutic effect, although the toxicity of ^{131}I -MIBG is a concern. For such high-dose therapy, ^{76}Br -MBBG would be useful not only for patient selection but also for evaluation of tumor and organ dosimetry, which would help in dose optimization and the prediction of side effects.

CONCLUSION

In the present study, MBBG showed a higher level of tumor accumulation than did MIBG. The tumor uptake of MBBG correlated well with that of MIBG but not with that of ^{18}F -FDG. In PET studies, ^{76}Br -MBBG provided a clear image, with high sensitivity, and its accumulation pattern was distinct from that of ^{18}F -FDG. These results indicate that ^{76}Br -MBBG is a potential tracer for imaging NET-expressing neuroendocrine tumors and may provide useful information for determining a treatment plan that incorporates ^{131}I -MIBG therapy.

ACKNOWLEDGMENTS

We thank Hiroyuki Suto and the staff of Takasaki Ion Accelerators for Advanced Radiation Application for operating the azimuthally varying field cyclotron. We also thank Dr. Satoshi Watanabe for preparing the no-carrier-added radiobromine and Dr. Shinji Yamamoto for performing the histologic staining. We thank Fujifilm RI Pharma Co., Ltd., for kindly providing ^{125}I -MIBG. Finally, we thank the staff of the Medical Radioisotope Application Group at the Japan Atomic Energy Agency and the staff of the Departments of Diagnostic Radiology and Nuclear Medicine at Gunma University Graduate School of Medicine for their cooperation and helpful input. This study was supported in part by a grant-in-aid for the 21st Century COE Program from the Ministry of Education, Sports, and Culture of Japan and a grant-in-aid for Young Scientists, (B) 21791227, from the Japan Society for the Promotion of Science.

REFERENCES

1. Wieland DM, Wu J, Brown LE, Mangner TJ, Swanson DP, Beierwaltes WH. Radiolabeled adrenergic neuron-blocking agents: adrenomedullary imaging with [^{131}I]iodobenzylguanidine. *J Nucl Med.* 1980;21:349–353.
2. Wieland DM, Brown LE, Rogers WL, et al. Myocardial imaging with a radioiodinated norepinephrine storage analog. *J Nucl Med.* 1981;22:22–31.
3. Rufini V, Shulkin B. The evolution in the use of MIBG in more than 25 years of experimental and clinical applications. *Q J Nucl Med Mol Imaging.* 2008;52:341–350.
4. Chrisoulidou A, Kaltsas G, Ilias I, Grossman AB. The diagnosis and management of malignant pheochromocytoma and paraganglioma. *Endocr Relat Cancer.* 2007;14:569–585.
5. Gedik GK, Hoefnagel CA, Bais E, Olmos RA. ^{131}I -MIBG therapy in metastatic pheochromocytoma and paraganglioma. *Eur J Nucl Med Mol Imaging.* 2008;35:725–733.
6. Nwosu AC, Jones L, Vora J, Poston GJ, Vinjamuri S, Pritchard DM. Assessment of the efficacy and toxicity of ^{131}I -metaiodobenzylguanidine therapy for metastatic neuroendocrine tumours. *Br J Cancer.* 2008;98:1053–1058.
7. Sharp SE, Shulkin BL, Gelfand MJ, Salisbury S, Furman WL. ^{123}I -MIBG scintigraphy and ^{18}F -FDG PET in neuroblastoma. *J Nucl Med.* 2009;50:1237–1243.
8. Shulkin BL, Thompson NW, Shapiro B, Francis IR, Sisson JC. Pheochromocytomas: imaging with 2-[fluorine-18]fluoro-2-deoxy-D-glucose PET. *Radiology.* 1999;212:35–41.
9. Taniguchi K, Ishizu K, Torizuka T, et al. Metastases of predominantly dopamine-secreting pheochromocytoma that did not accumulate meta-iodobenzylguanidine: imaging with whole body positron emission tomography using ^{18}F -labelled deoxyglucose. *Eur J Surg.* 2001;167:866–870.
10. Ezuddin S, Fragkaki C. MIBG and FDG PET findings in a patient with malignant pheochromocytoma: a significant discrepancy. *Clin Nucl Med.* 2005;30:579–581.
11. Takano A, Oriuchi N, Tsushima Y, et al. Detection of metastatic lesions from malignant pheochromocytoma and paraganglioma with diffusion-weighted magnetic resonance imaging: comparison with ^{18}F -FDG positron emission tomography and ^{123}I -MIBG scintigraphy. *Ann Nucl Med.* 2008;22:395–401.
12. Rowland DJ, McCarthy TJ, Welch MJ. Radiobromine for imaging and therapy. In: Welch MJ, Redvanly CS, eds. *Handbook of Radiopharmaceuticals: Radiochemistry and Applications.* West Sussex, U.K.: John Wiley & Sons; 2003:441–465.
13. Loc'h C, Mardon K, Valette H, et al. Preparation and pharmacological characterization of [^{76}Br]-meta-bromobenzylguanidine ([^{76}Br]MBBG). *Nucl Med Biol.* 1994;21:49–55.
14. Valette H, Loc'h C, Mardon K, et al. Bromine-76-metabromobenzylguanidine: a PET radiotracer for mapping sympathetic nerves of the heart. *J Nucl Med.* 1993;34:1739–1744.
15. Clerc J, Mardon K, Galons H, et al. Assessing intratumor distribution and uptake with MBBG versus MIBG imaging and targeting xenografted PC12-pheochromocytoma cell line. *J Nucl Med.* 1995;36:859–866.

16. Tolmachev V, Löfvqvist A, Einarsson L, Schultz J, Lundqvist H. Production of ⁷⁶Br by a low-energy cyclotron. *Appl Radiat Isot.* 1998;49:1537–1540.
17. Nanni C, Leo DK, Tonelli R, et al. FDG small animal PET permits early detection of malignant cells in a xenograft murine model. *Eur J Nucl Med Mol Imaging.* 2007;34:755–762.
18. Kimura N, Watanabe T, Noshiro T, Shizawa S, Miura Y. Histological grading of adrenal and extra-adrenal pheochromocytomas and relationship to prognosis: a clinicopathological analysis of 116 adrenal pheochromocytomas and 30 extra-adrenal sympathetic paragangliomas including 38 malignant tumors. *Endocr Pathol.* 2005;16:23–32.
19. Bruhlmeier M, Roelcke U, Blauenstein P, et al. Measurement of the extracellular space in brain tumors using ⁷⁶Br-bromide and PET. *J Nucl Med.* 2003;44:1210–1218.
20. Gudjonsson O, Bergstrom M, Kristjansson S, et al. Analysis of ⁷⁶Br-BrdU in DNA of brain tumors after a PET study does not support its use as a proliferation marker. *Nucl Med Biol.* 2001;28:59–65.
21. Berry CR, Garg PK, DeGrado TR, et al. Para-[¹⁸F]fluorobenzylguanidine kinetics in a canine coronary artery occlusion model. *J Nucl Cardiol.* 1996;3:119–129.
22. Garg PK, Garg S, Zalutsky MR. Synthesis and preliminary evaluation of para- and meta-[¹⁸F]fluorobenzylguanidine. *Nucl Med Biol.* 1994;21:97–103.
23. Westerberg G, Långström B. Synthesis of meta-iodobenzyl [¹¹C]guanidine. *J Labelled Comp Radiopharm.* 1997;39:525–529.
24. Vaidyanathan G, Affleck DJ, Zalutsky MR. Validation of 4-[fluorine-18]fluoro-3-iodobenzylguanidine as a positron-emitting analog of MIBG. *J Nucl Med.* 1995;36:644–650.
25. Moroz MA, Serganova I, Zanzonico P, et al. Imaging hNET reporter gene expression with I-124-MIBG. *J Nucl Med.* 2007;48:827–836.
26. Ott RJ, Tait D, Flower MA, Babich JW, Lambrecht RM. Treatment planning for I-131 metaiodobenzylguanidine radiotherapy of neural crest tumors using I-124 metaiodobenzylguanidine positron emission tomography. *Br J Radiol.* 1992;65:787–791.
27. Hoegerle S, Nitzsche E, Altehoefer C, et al. Pheochromocytomas: detection with ¹⁸F DOPA whole body PET-initial results. *Radiology.* 2002;222:507–512.
28. Imani F, Agopian VG, Auerbach MS, et al. ¹⁸F-FDOPA PET and PET/CT accurately localize pheochromocytomas. *J Nucl Med.* 2009;50:513–519.
29. Taieb D, Tessonnier L, Sebag F, et al. The role of ¹⁸F-FDOPA and ¹⁸F-FDG-PET in the management of malignant and multifocal pheochromocytomas. *Clin Endocrinol (Oxf).* 2008;69:580–586.
30. Ilias I, Chen CC, Carrasquillo JA, et al. Comparison of 6-¹⁸F-fluorodopamine PET with ¹²³I-metaiodobenzylguanidine and ¹¹¹In-pentetreotide scintigraphy in localization of nonmetastatic and metastatic pheochromocytoma. *J Nucl Med.* 2008;49:1613–1619.
31. Ilias I, Pacak K. Current approaches and recommended algorithm for the diagnostic localization of pheochromocytoma. *J Clin Endocrinol Metab.* 2004;89:479–491.
32. Ilias I, Yu J, Carrasquillo JA, et al. Superiority of 6-[¹⁸F]-fluorodopamine positron emission tomography versus [¹³¹I]-metaiodobenzylguanidine scintigraphy in the localization of metastatic pheochromocytoma. *J Clin Endocrinol Metab.* 2003;88:4083–4087.
33. Pacak K, Eisenhofer G, Carrasquillo JA, Chen CC, Li ST, Goldstein DS. 6-[¹⁸F] fluorodopamine positron emission tomographic (PET) scanning for diagnostic localization of pheochromocytoma. *Hypertension.* 2001;38:6–8.
34. Adams S, Baum R, Rink T, Schumm-Drager PM, Usadel KH, Hor G. Limited value of fluorine-18 fluorodeoxyglucose positron emission tomography for the imaging of neuroendocrine tumours. *Eur J Nucl Med.* 1998;25:79–83.
35. Scholz T, Eisenhofer G, Pacak K, Dralle H, Lehnert H. Clinical review: current treatment of malignant pheochromocytoma. *J Clin Endocrinol Metab.* 2007;92:1217–1225.
36. Gonias S, Goldsby R, Matthy KK, et al. Phase II study of high-dose [¹³¹I] metaiodobenzylguanidine therapy for patients with metastatic pheochromocytoma and paraganglioma. *J Clin Oncol.* 2009;27:4162–4168.